DOI 10.5162/irs2015/P2

Investigation of InAsSbP Quantum Dot Mid-Infrared Sensors

V.G. Harutyunyan, K.M. Gambaryan, V.M. Aroutiounian
Department of Physics of Semiconductors and Microelectronics, Yerevan State University,
1 A. Manoogian, Yerevan 0025, Armenia
E-mail: harutyunyan@ysu.am

Abstract

This work presents the results of investigation of low bias mid-IR photoconductive cell (PCC) with quantum dots. Self-assembled InAsSbP nanostructures were grown on InAs(100) substrate by modified liquid phase epitaxy. Hysteresis with remnant capacitance of 0.483 pF and contra-directional oscillations on the PCC's capacitance–voltage characteristic at 78 K were observed. Additionally, peaks at 3.48 µm, 3.68 µm and 3.89 µm on room temperature photoresponse spectrum of quantum dot photoconductive cell were detected. Room temperature photo-sensing properties were investigated under monochromatic irradiation of 3.39 µm as well. At irradiation power density of 0.07 W/cm^2 the surface resistance of the PCC was reduced up to 10 %. In the case of 8 mV applied voltage, the current responsivity of 0.2 mA/W was measured.

Key words: InAsSbP quantum dots, Mid-IR, Photoconductive Cells, Low bias, Responsivity.

1. Introduction

The importance of the mid-IR range attributes to the transmission window of the atmosphere, absorption spectra of some industrial gases, etc. To satisfy the demands of state-of-the-art infrared photodetectors, quantum well infrared photodetectors (QWIP) and quantum dot infrared photodetectors (QDIP) are of great interest. QDIPs are predicted to have superior performances compared to QWIPs [1-2] such as sensitivity to normal incidence infrared radiation, low dark current, high responsivity and detectivity. Many semiconductor material systems, such as InGaAs/GaAs, InAsSb/GaAs, InAs/GaAs, etc., were investigated for QDIPs [3-5]. HgCdTe (MCT) is a well-established solid solution, which has been the dominant system for mid- and long-infrared photodetectors. However, MCT suffers from instability and non-uniformity problems over larger area due to the high Hg vapor pressure. Theoretical studies predicted that only type-II superlattice photodiodes and QDIPs are expected to compete with HgCdTe photodiodes [6]. InAs-InSb-InP system could be discussed as an alternative material system for mid-IR applications. InAsSbP quaternary alloy was also successfully applied for nucleation of quantum dots (QDs). In the first experiment to grow nanostructures, GaAs was used as a substrate [7]. QDs were characterized by photoluminescence measurements at 4 K temperature. Due to QDs, photoluminescence peak at 1.65 µm was observed. Recently, InAsSbP QDs were successfully grown also on InAs substrates [8-12].

In this paper we report our efforts to grow InAsSbP QDs for mid-IR applications. Quantum dot mid-IR photodetectors are fabricated in the form of photoconductive cells (PCC) made of InAs(100) substrate and QDs grown on it. Electrophysical and optoelectronic properties of the photodetectors are presented.

2. Experiment

To grow QDs, a modified liquid phase epitaxy (MLPE) was used. In our LPE process melted In (7N) was used as a solvent, InAs, InP and Sb (6N) were used as solutes. Lattice mismatch of 2% between n-InAs(100) substrate with thickness of 400 µm and wetting layer was chosen to provide the growth of InAsSbP nanostructures in Stranski-Krastanov mode [13, 14]. An atomic force microscope (AFM-Asylum Research MFP-3D) was employed to investigate the surface morphology, size distribution and density of quantum dots. Au/Cr evaporation was performed to obtain contacts on the surface of the nanostructures. Actually, fabricated photoconductive cell (PCC) consists of InAs substrate, unencapsulated InAsSbP QDs and contacts (Fig. 1). The active area of the photoconductive cell is 0.83 mm^2.

Capacitance-voltage (C–V) characteristics were investigated using high precision capacitance spectrometry (QuadTech-1920 precision LCR meter). Mid-IR photoresponse spectra were measured by IRS-21 spectrometer. He-Ne laser was used as a source of 3.39 µm irradiation.

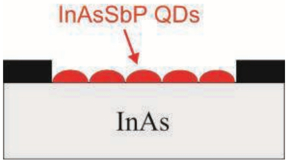

Fig. 1. Schematic of the photoconductive cell with QDs.

3. Results and discussion

The AFM image of grown InAsSbP quantum dots obtained by AFM is presented in Fig. 2. The average surface density of QDs was found to be 7×10^9 cm^{-2}. The heights of QDs ranges from 5 nm to 23 nm and widths from 10 nm to 50 nm.

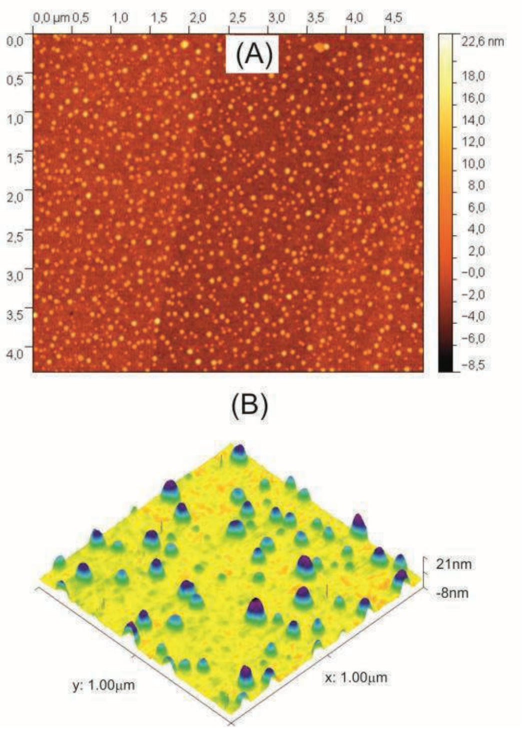

Fig. 2. AFM images of unencapsulated InAsSbP QDs grown on InAs(100): A - plane view, B - oblique view.

Figure 3 shows the dark current–voltage (I–V) characteristic of the PCC. Nonlinear behavior is found at around ~60 mV voltage. The results of the C–V characterization performed at 78 K and 10^6 Hz frequency is presented in Fig. 4. The measurements were performed by increasing signal voltage from 0 V up to 0.9 V with further decreasing back to 0 V as denoted by arrows in the Fig. 4. Also, it can be seen that oscillations on C–V curve are observed. Oscillations observed during increasing voltage are opposite-directed to the oscillations observed during further decreasing of the voltage. Additionally, as we can see from Fig. 4, capacitance hysteresis with remnant capacitance of ΔC=0.483 pF is observed. We assume that opposite–directed oscillations revealed on C-V curve occur due to the structure's total charge oscillations, which cause by the depletion and occupation of the QDs energy levels. Detected hysteresis can be explained by the remnant polarization in the structure due to spatial separation of the charge carriers in type-II InAsSbP QDs [8], which conserved after shut off the applied voltage.

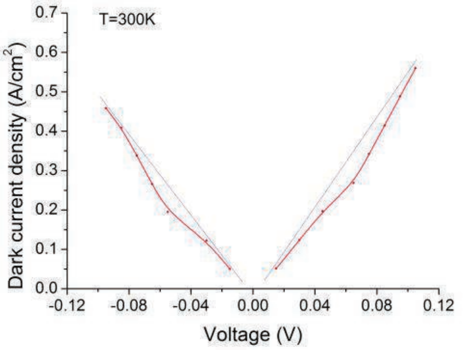

Fig. 3. Dark current density of the PCC versus bias voltage.

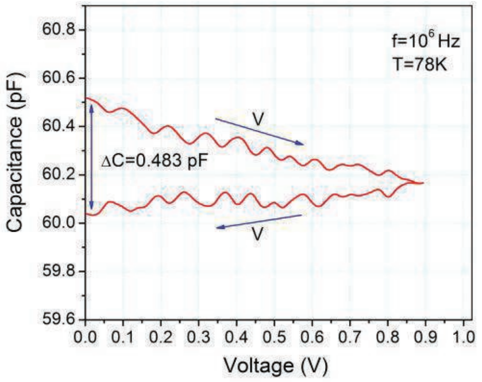

Fig. 4. Capacitance–voltage characteristic of the PCC.

For photoresponse measurements a testing infrared photodetector (TIP) was fabricated and used. The TIP is a traditional photoconductive cell made of InAs bulk crystal (without QDs). The photoresponse spectra of the samples at room temperature were investigated applying 2 mV bias. For TIP only one peak at 3.48 µm due to band-to-band transitions in InAs (Eg=0.355 eV) was observed (Fig. 5). It can be obviously seen that the sample with QDs (PCC) in comparison with the sample without QDs has photoresponse spectrum extended to longer wavelengths up to 4 µm with a narrow peak at 3.48 µm. Also, additional two peaks observed at 3.68 µm and 3.89 µm longer wavelengths. These last mentioned peaks are attributed to the transitions in sub-bandgap levels created by QDs.

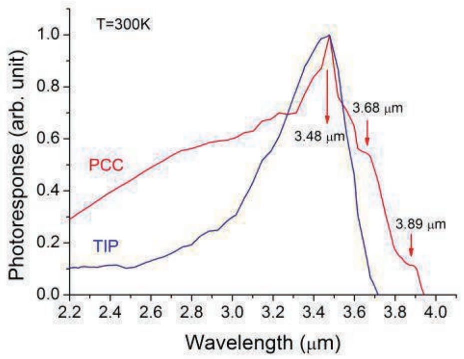

Fig. 5. Photoresponse spectra of the TIP and PCC at room temperature.

The surface resistance of the samples was also investigated under irradiation with wavelength of 3.39 µm. The relative surface resistance change of the PCC versus power density is plotted in Fig. 6. At power density of 0.07 W/cm^2 the resistance of the PCC was reduced by 7 %.

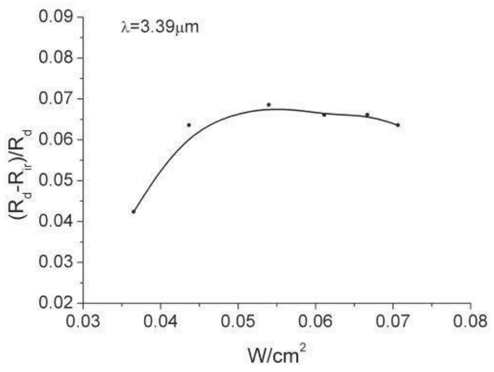

Fig. 6. Surface resistance change vs power density. R_d is the dark resistance and R_{ir} is the resistance under irradiation.

Meanwhile, the surface the TIP at the same density was reduced by resistance of 2%. So, due to the growth of InAsSbP QDs, the resistance change sensitivity of the PCC is increased by 3.5 times. The current responsivity of the PCC was investigated at power density of 0.05 W/cm^2 (Fig. 7). Current responsivity of 0.2 mA/W was achieved at low bias of 8 mV, which exceeds the responsivity of the TIP by 20 times at the same power density and bias. So, fabricated photoconductive cells with InAsSbP quantum dots are important for low bias operation at mid-IR range. Reported results could be important to develop the idea of photoconductive cells with quantum dots for next generation infrared devices.

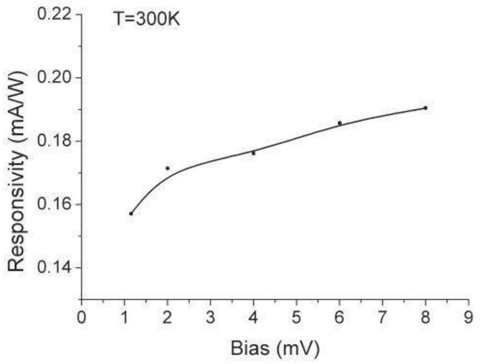

Fig. 7. Current responsivity of the PCC as a function of bias.

4. Conclusion

A low bias mid-IR photoconductive cell with InAsSbP QDs was fabricated. Nonlinear current-voltage behavior was found at room temperature. The sample was investigated by C–V characterization as well. In result, specific opposite-directed oscillations and hysteresis with remnant capacitance of ΔC=0.483 pF were observed at 78 K temperature. PCC's room temperature photoresponse spectrum is extended to longer wavelengths up to 4 µm. Besides red shift, two additional peaks were observed at 3.68 µm and 3.89 µm wavelengths. It was shown that under irradiation of 3.39 µm, PCC's resistance changes 3.5 times more than that of TIP. Applying 8 mV bias, current responsivity of 0.2 mA/W for PCC was measured. This value exceeds the TIP's responsivity by 20 times. Thus, the photodetector with InAsSbP QDs is considered to be operating in mid-IR range at low bias.

Acknowledgments

This work was performed in the frame of MES-BMBF-STC-2012 (№ 12GE-015) Armenian-German joint project, as well as in the frame of award № YSSP-13-08 supported by the National Foundation of Science and Advanced Technologies (NFSAT), Youth Foundation of Armenia (AYF) and CRDF Global.

References

[1] V. Ryzhii, The theory of quantum-dot infrared phototransistors, *Semiconductor Science and Technolology*. 11, 759-765 (1996); doi: 10.1088/0268-1242/11/5/018.

[2] J. Phillips, Evaluation of the fundamental properties of quantum dot infrared detectors,

Journal of Applied Physics. 91, 4590-4594 (2002); doi: 10.1063/1.1455130

[3] P. Bhattacharya, X.H. Su, S. Chakrabarti, G. Ariyawansa, A.G.U. Perera, Characteristics of a Tunneling Quantum-dot Infrared Photodetector Operating at Room Temperature, *Applied Physics Letters* 86, 191106-1–1191106-3 (2005); doi: 10.1063/1.1923766

[4] J. He, C.J. Reyner, B.L. Liang, K. Nunna, D.L. Huffaker, N. Pavarelli, K. Gradkowski, T.J. Ochalski, G. Huyet, V.G. Dorogan, Y.I. Mazur, G.J. Salamo, Band alignment tailoring of InAs1-xSbx/GaAs quantum dots: Control of type I to type II transition, *Nano Letters* 10, 3052-3056, (2010); 10.1021/nl102237n

[5] Yan-Feng Lao, Seyoum Wolde, A. G. Unil Perera, Y. H. Zhang, T. M. Wang, H. C. Liu, J. O. Kim, Ted Schuler-Sandy Zhao-Bing Tian, S. S. Krishna, InAs/GaAs p-type quantum dot infrared photodetector with higher efficiency, *Applied Physics Letters* 103, 241115-1_241115-4 (2013); doi: 10.1063/1.4846555

[6] P. Martyniuk, A. Rogalski, Quantum-dot infrared photodetectors: Status and outlook, *Progress in Quantum Electronics* 32, 89-120 (2008); doi: 10.1016/j.pquantelec.2008.07.001

[7] A. Krier, Z. Labadi, A. Hammiche, InAsSbP quantum dots grown by liquid phase epitaxy, *Journal of Physics D: Applied Physics* 32, 2587-2589 (1999); doi: 10.1088/0022-3727/32/20/301

[8] K.M. Gambaryan, Interaction and Cooperative Nucleation of InAsSbP Quantum, Dots and Pits on InAs(100) Substrate, *Nanoscale Research. Letters*. 5, 587-591 (2010); doi: 10.1007/s11671-009-9510-8

[9] K.M. Gambaryan, V.M. Aroutiounian, V.G. Harutyunyan, O. Marquardt, P.G. Soukiassian, Room temperature magnetoelectric properties of type-II InAsSbP quantum dots and nanorings, *Applied Physics Letters* 100, 033104-1_ 033104-4 (2012); doi:10.1063/1.3676437

[10] K.M. Gambaryan, V.M. Aroutiounian, V.G. Harutyunyan, Nucleation features and energy levels of type-II InAsSbP quantum dots grown on InAs(100) substrate, *Applied Physics Letters* 101, 093103-1_093103-5 (2012); doi: 10.1063/1.4748574

[11] K.M. Gambaryan, V.M. Aroutiounian, V.G. Harutyunyan, Photovoltaic and optoelectronic properties of InAs(1 0 0)-based photoconductive cells with quantum dots and nanopits, *Infrared Physics & Technology* 54, 114-120 (2011); doi: 10.1016/j.infrared.2011.01.005

[12] V. Harutyunyan, K. Gambaryan, V. Aroutiounian, Novel narrow band-gap InAsSbP-based quantum dot mid-infrared photodetectors: fabrication, optoelectronic and electrophysical properties, *Journal of Nanoscience and Nanotechnology* 13, 799-803 (2013); doi: 10.1166/jnn.2013.6066.

[13] I.N. Stranski, L. Krastanov. Zur theorie der orientierten ausscheidung von Sitz. Ber. Akad. Wiss. Math.-naturwiss. Kl. Abt. IIb 146:797-810 (1938)

[14] . A. Baskaran, P. Smerek, Mechanisms of Stranski-Krastanov growth, J*ournal of Applied Physics* 111, 044321-1_044321-6 (2012); doi: 10.1063/1.3679068

[15] O. Marquardt, T. Hickel, J. Neugebauer, K.M. Gambaryan, V.M. Aroutiounian, Growth process, characterization, and modeling of electronic properties of coupled InAsSbP nanostructures, *Journal of Applied Physics* 110, 043708-1_043708-6 (2011); doi: 10.1063/1.3624621.